npg

www.nature.com/bjp

Electrophysiological evidence for a gradient of G protein-gated K^+ current in adult mouse atria

[1]Alan E. Lomax, [1]Robert A. Rose & *,[1,2]Wayne R. Giles

[1]Department of Physiology and Biophysics, University of Calgary, Alberta, Canada T2N 4N1 and [2]Department of Bioengineering, University of California, San Diego, 9500 Gilman Drive, La Jolla, CA 92093-0412, U.S.A.

1 Whole cell current and voltage clamp techniques were used to examine the properties of acetylcholine-sensitive K^+ current (IKACh) in myocytes from adult mouse atrium. Superfusion of a maximal dose of carbachol (CCh; $10\,\mu M$) caused a substantial increase in K^+ current in all myocytes examined.

2 The current–voltage ($I–V$) relation of maximally activated IKACh exhibited weak inward rectification. Consequently, CCh increased the amount of depolarising current necessary to evoke action potentials (APs), and APs evoked in CCh had significantly shorter durations than control APs ($P < 0.05$).

3 The effects of CCh on K^+ current and on AP properties were blocked by the muscarinic receptor antagonist methoctramine ($1\,\mu M$). ACh ($10\,\mu M$) activated a K^+ current with identical properties to that activated by CCh, as did the A_1 receptor agonist adenosine ($100\,\mu M$).

4 Right atrial myocytes had significantly more IKACh than left atrial myocytes ($P < 0.05$), regardless of whether IKACh was evoked by superfusion of muscarinic or A_1 receptor agonists. IKACh current density was significantly higher in SA node myocytes than either right or left atrial myocytes.

5 These data identify a gradient of IKACh current density across the supraventricular structures of mouse heart. This gradient, combined with the heterogeneous distribution of parasympathetic innervation of the atria, may contribute to the proarrhythmic ability of vagal nerve stimulation to augment dispersion of atrial refractoriness.

British Journal of Pharmacology (2003) **140**, 576–584. doi:10.1038/sj.bjp.0705474

Introduction

The ability of acetylcholine (ACh) to increase K^+ conductance in cardiac tissue has been the subject of detailed investigations for many years (reviewed by Wickman & Clapham, 1995; Yamada et al., 1998). ACh increases K^+ conductance by binding muscarinic receptors, which triggers the activation of pertussis toxin-sensitive G-proteins. The activated $G\alpha$ and $G\beta\gamma$ subunits exert multiple effects on various enzymes and ion channels, including voltage- and time-dependent Ca^{2+} channels and the G-protein-gated K^+ channel (IKACh; Wickman & Clapham, 1995; Yamada et al., 1998). IKACh is an inward rectifier K^+ channel comprised of a tetramer of the α subunits Kir 3.1/GIRK1 and Kir 3.4/GIRK4 (Dascal et al., 1993; Kubo et al., 1993; Krapivinsky et al., 1995; Bettahi et al., 2002). It is now well established that IKACh can be activated *via* a membrane-delimited pathway involving a direct interaction of $G\beta\gamma$ with the α subunits that comprise this K^+ channel (Logothetis et al., 1987). Other ligands that bind pertussis toxin-sensitive G-protein-coupled receptors, such as adenosine

and sphingosine-1-phosphate, can also activate IKACh (Yamada et al., 1998).

Atrial tachyarrhythmias often result from re-entrant excitation of atrial myocardium. This re-entry is thought to be due to inhomogeneities of refractoriness in adjacent areas of atrial tissue (e.g. Boutjdir et al., 1986). Myocardial refractoriness is determined by a combination of the recovery from inactivation of voltage- and time-dependent sodium current (I_{Na}) and residual activation of time- and voltage-dependent and G-protein-gated-gated K^+ currents. Recovery from inactivation of I_{Na} proceeds rapidly only at hyperpolarised membrane potentials; thus, its time course is related to the duration of the action potential (AP) and the resting membrane potential (RMP). Several recent studies have identified heterogeneous expression of voltage- and time-dependent K^+ channels, which influence AP repolarisation and the RMP, between left and right atrium (Li et al., 2001; Lomax et al., 2003). This heterogeneity may lead to dispersion of refractoriness and contribute to atrial re-entry (Wirth & Knobloch, 2001; Knobloch et al., 2002; Nattel, 2002).

The interaction of sympathetic and parasympathetic branches of the autonomic nervous system plays a key role in

modulating atrial refractoriness, and recent work has demonstrated that heterogeneous innervation of the atria by cholinergic parasympathetic nerve terminals can cause sufficient dispersion of refractoriness to trigger re-entry (Olgin *et al.*, 1998; Hirose *et al.*, 2002a). Moreover, infusion or perfusion of ACh, carbamylcholine (CCh) or adenosine can also trigger atrial tachyarrhythmias in humans, sheep and mice (Coumel, 1996; Kovoor *et al.*, 2001; Mansour *et al.*, 2001). These proarrhythmic effects are observed consistently, despite the fact that infused or perfused substances can reach atrial myocardium in a uniform manner. It has also been reported that fibrillation could not be induced in the atria of mice that lack IKACh, suggesting a key role for IKACh in the generation of atrial fibrillation (Kovoor *et al.*, 2001). For these reasons, we developed the working hypothesis that the role of IKACh in initiating and maintaining atrial fibrillation is due to heterogeneity of IKACh expression patterns which, in turn, could lead to spatial dispersion of atrial refractoriness. Accordingly, the aim of the present study was to examine whether expression of IKACh in adult mouse atria is heterogeneous.

Methods

These experiments were conducted using acutely dissociated single atrial and sinoatrial (SA) node myocytes from 8 to 10-week-old male C57BL6 mice. The methodology conforms with the Guide for the Care and Use of Laboratory Animals published by the National Institutes of Health (NIH publication No. 85–23, revised 1996) and with University of Calgary guidelines. Atrial myocytes were dissociated as follows: Beating hearts were removed from mice following methoxyflurane inhalation anaesthesia and cervical dislocation. Left and right atria were then dissected away from the remaining supraventricular structures in a Tyrodes solution containing (mM): NaCl, 140; KCl, 5.4; MgCl$_2$, 1; CaCl$_2$, 1.8; HEPES, 5; D-glucose, 5.5 and heparin, 10 i.u. ml^{-1} that was warmed to 35°C (pH = 7.4 with NaOH). Left and right atria were then separated and cut into 10 strips for enzymatic treatment.

Atrial tissue strips were transferred to a solution containing in mM: NaCl, 140; KCl, 5.4; CaCl$_2$, 0.2; MgCl$_2$, 0.5; KH$_2$PO$_4$, 1.2; taurine, 50; D-glucose, 5.5, bovine serum albumin (BSA), 1 mg ml^{-1}; HEPES, 5; pH was adjusted to 7.4. Following three washes in this low Ca^{2+}-containing solution, tissue strips were digested by adding collagenase type II (225 U ml^{-1}, Worthington Biochemical Corporation, Lakewood NJ, U.S.A.), elastase (1.8 U ml^{-1}, Worthington) and protease type XIV (0.35 U ml^{-1}, Sigma Chemical Co., Oakville, Ontario, Canada) to the solution. Enzymatic digestion took place for 30–35 min at 35°C, with manual agitation every 5 min. The tissue was then washed five times in a modified Kraftbrühe (KB) solution containing (mM): potassium glutamate, 100; potassium aspartate, 10; KCl, 25; KH$_2$PO$_4$, 10; MgSO$_4$, 2; taurine, 20; creatine base, 5; EGTA, 0.5; HEPES, 5; D-glucose, 20 and BSA, 1 mg ml^{-1} (pH adjusted to 7.2 with KOH). Following this washing procedure, single atrial myocytes were isolated by gentle trituration at room temperature using a fire-polished Pasteur pipette with an inner diameter of 3 mm. Aliquots of this cell suspension were examined using a phase-contrast microscope (Zeiss ID 03) as trituration progressed. Trituration was continued until an acceptable yield of single atrial myocytes was achieved, usually within 10 min. Myocytes were

then readapted to normal extracellular Ca^{2+} concentrations by the addition of solution containing 10 mM NaCl and 1.8 mM CaCl$_2$ followed by normal Tyrodes solution containing 1 mg ml^{-1} BSA. Isolated myocytes were then stored in a solution containing (mM): NaCl, 100; KCl, 35; CaCl$_2$, 1.3; MgCl$_2$, 0.7; potassium glutamate, 14; KH$_2$PO$_4$, 2; taurine 2 and BSA, 1 mg ml^{-1}, until they were used in electrophysiology experiments.

Single myocytes from the SA node region were dissociated according to the methods of Mangoni and Nargeot (2001). In summary, mice were anaesthetised with methoxyflurane and cervically dislocated. The heart was then excised and placed in Tyrodes solution containing in mM: NaCl, 140; KCl, 5.4; KH$_2$PO$_4$, 1.2; MgCl$_2$, 1.0; CaCl$_2$, 1.8; glucose, 5.55; HEPES, 5 (pH = 7.4 with NaOH) at 35°C. The SA node region of the heart was isolated by separating the atria from the ventricles, cutting open the superior and inferior vena cavae, and pinning the tissue so that the crista terminalis could be visualised. The SA node was demarcated by boundaries consisting of the crista terminalis, the interatrial septum and the openings of the two great veins. This SA node region was cut into three strips, which were transferred to a 'low-Ca^{2+}' solution containing in mM: NaCl, 140; KCl, 5.4; KH$_2$PO$_4$, 1.2; CaCl$_2$, 0.2; taurine, 50; glucose, 18.5; HEPES, 5; bovine serum albumin, 1 mg ml^{-1} (pH = 6.9 with NaOH). SA node tissue strips were digested by placing them in 5 ml of this solution containing collagenase (225 U ml^{-1}, Worthington type II), elastase (1.4 U ml^{-1}, Worthington) and protease (0.8 U ml^{-1}, Sigma type XIV) for 20–23 min. Following this, the tissue was transferred to 5 ml of KB solution and single cells were released by up to 10 min trituration at 35°C using a pipette with an inner diameter of 3 mm. This procedure yielded a sufficient number of SA node myocytes that were then readapted by gradually exposing the myocytes to a physiological concentration of Ca^{2+} in the same way that atrial myocytes were readapted. SA node myocytes were identified by their morphology and their spontaneous activity, and by measuring the hyperpolarisation-activated nonselective cation current, I_f, which is characteristic of SA node but not atrial myocytes, during a 2 s voltage clamp step from −35 to −135 mV.

Electrophysiology

For electrophysiological recordings, an aliquot of cell suspensions from either left or right atria or from SA node was allowed to settle for 15 min in a modified 35 mm Petri dish (volume = 250 μl) that was mounted on the stage of a Nikon Diaphot inverted microscope. Myocyte suspensions were then continuously superfused at room temperature (22°C) with Tyrodes solution of the following composition (mM): NaCl, 140; KCl, 5.4; CaCl$_2$, 1; MgCl$_2$, 1; HEPES, 10 and D-glucose, 5.5 (pH adjusted to 7.4 with NaOH). The superfusion flow rate was 2 ml min^{-1} unless stated otherwise. Patch pipettes were made from borosilicate glass (World Precision Instruments Inc., Sarasota, FL, U.S.A.) using a P-87 Flaming/Brown pipette puller (Sutter Instruments, Novato, CA, U.S.A.). These pipettes had resistances between 1.5 and 4 MΩ when filled with solution of the following composition (in mM): KCl, 130; NaCl, 12; CaCl$_2$, 1; MgCl$_2$, 1; dipotassium salt of ATP, 4; EGTA, 10; GTP, 0.2; HEPES, 10. pH was adjusted to 7.2 by the addition of KOH.

Whole cell voltage clamp and current clamp experiments were carried out using an Axopatch 200 B patch clamp

amplifier, interfaced to a Digidata 1322A analog to digital converter that was driven by Clampex 8.1 software (all from Axon Instruments Inc., Foster City, CA, U.S.A.). Acquired data were recorded to the hard drive of a personal computer and stored for *post hoc* analysis, using the pClamp suite of software (Axon Instruments) and Origin 4.1 (Microcal Software Inc., Northampton, MA, U.S.A.). The capacitance of each myocyte was measured by integrating the capacitive current evoked during 5 mV depolarising steps from a holding potential of -75 mV. Current amplitudes recorded in each myocyte were normalised to the cell capacitance (pA pF^{-1}). Whole cell experiments proceeded only if the series resistance was less than 15 MΩ. Series resistance was compensated electronically by 85%. As voltage errors resulting from uncompensated series resistance were very small, no corrections were applied.

Two voltage clamp protocols were utilised to examine the current voltage ($I-V$) relation of IKACh. One protocol consisted of a series of voltage steps in 10 mV increments between -115 and 45 mV from a holding potential of -75 mV. A ramp protocol was also used to determine the $I-V$ relation of IKACh; the membrane potential was changed from 45 to -140 mV over the course of 1 s. The holding potential was -75 mV.

Atrial APs were recorded under control conditions in response to 0.3–0.6 nA depolarising current pulses that lasted 4 ms using the Axopatch 200 B amplifier in current clamp mode. The amplitude of stimulus current required to elicit APs with stable latencies was noted. Stimuli were applied at 1 Hz, and the RMP and AP durations from the peak to the 50 and 90% repolarisation level (APD$_{50}$ and APD$_{90}$) were measured. A total of 60 APs were recorded per myocyte, before superfusion with any drugs commenced, and the final 30 APs were averaged and analysed to derive the control APD$_{50}$ and APD$_{90}$ for that myocyte. During superfusion of CCh, the stimulus current needed to evoke APs with stable latencies increased. Stimulus current was increased sufficiently to evoke stable APs and then 60 APs were recorded. The final 30 APs in the presence of CCh were averaged and used to measure the APD$_{50}$ and APD$_{90}$.

CCh was prepared as a stock solution in distilled water, and adenosine was prepared as a stock solution in 1 M NaOH, on the day of each experiment. ACh was dissolved in distilled water and stored in frozen aliquots until the day of the experiment. CCh, adenosine and ACh were purchased from Sigma (St Louis, MO, U.S.A.). Stock solutions were diluted by a factor of at least 1000 by addition to the superfusate.

Statistical analysis

The data are presented as means±s.e.m. For comparison of electrophysiological parameters from left and right atria, two-tailed unpaired Student's *t*-tests were used. For analysis of the effects of pharmacological agents on currents and AP durations, paired two-tailed Student's *t*-tests were used. In each case, a probability of $P < 0.05$ was considered significant.

Results

Effects of CCh on K$^+$ current and AP characteristics

Figure 1 shows representative responses of three different atrial myocytes to superfusion of three different agonists that

activate IKACh. The membrane potential of these myocytes was held at -100 mV in the presence of 50 μM BaCl$_2$ (which blocks IK$_1$ but does not affect IKACh), while each agonist was superfused for 1 min at a flow rate of 5 ml min^{-1}. Several features of the responses are noteworthy: (1) The responses of the myocytes to maximal concentrations of ACh and CCh (panels a and c) rapidly desensitised to approximately 85% of maximal level, whereas the response of the myocyte to adenosine (panel b) did not desensitise. (2) The onset of the responses to muscarinic receptor agonists was much more rapid than the responses to adenosine. The slow onset of the responses to adenosine and the lack of desensitization are well-characterised phenomena (Wellner-Kienitz *et al.*, 2000). The responses shown below are characteristic of the responses observed in five other myocytes to ACh, seven other myocytes to adenosine and six other myocytes to CCh. Owing to the rapid desensitisation of the current responses to muscarinic agonists, steady-state (rather than peak) current responses were measured in subsequent experiments.

Figure 2 shows the properties of steady-state IKACh in mouse atrial myocytes, and describes the voltage clamp protocols that were used to examine it. The membrane potential was stepped in 10 mV increments between -115 and 45 mV, or was ramped from 45 to -140 mV, from a holding potential of -75 mV (see insets at top). The left- and right-hand panels compare the response of a single right atrial myocyte to both step and ramp protocols, respectively. Figure 2a and b show the voltage- and time-dependent currents recorded in response to these voltage clamp protocols under control conditions. In panels c and d, the response of the myocyte to identical protocols in the presence of a maximal dose of CCh (10 μM) is presented. The traces in control conditions were digitally subtracted from the traces in CCh to yield the CCh-sensitive difference currents shown in Figure 2e and f. Note the presence of IKACh tail currents, as have been previously described for mammalian and amphibian atrial myocytes (Noma & Trautwein, 1978; Simmons & Hartzell, 1987). The difference currents in Figure 2e and f represents IKACh, and both the voltage step and the ramp protocols can be used to obtain the $I-V$ relation, as seen in Figure 2g. The squares denote the current measured at the end of the voltage clamp steps, and the continuous line is derived from measurements of instantaneous current during the ramp protocol. Note that the $I-V$ relations are almost superimposable. Difference currents derived from ramp protocols
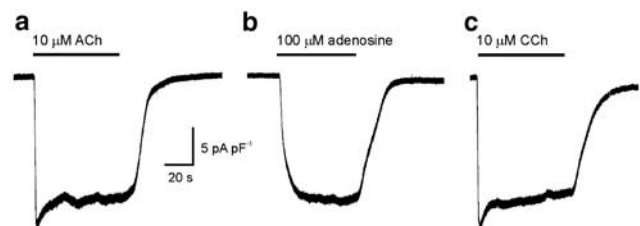

Figure 1 Time course of effects of muscarinic agonists and adenosine on K$^+$ current in myocytes from adult mouse atrium. (a–c) Examples of whole cell current change at -100 mV during superfusion with ACh, adenosine and CCh in three myocytes. Superfusion with muscarinic agonists caused an increase in inward K$^+$ current, followed by rapid desensitisation of the current response. In contrast, the K$^+$ current change in response to adenosine was slower in onset and did not desensitise appreciably.
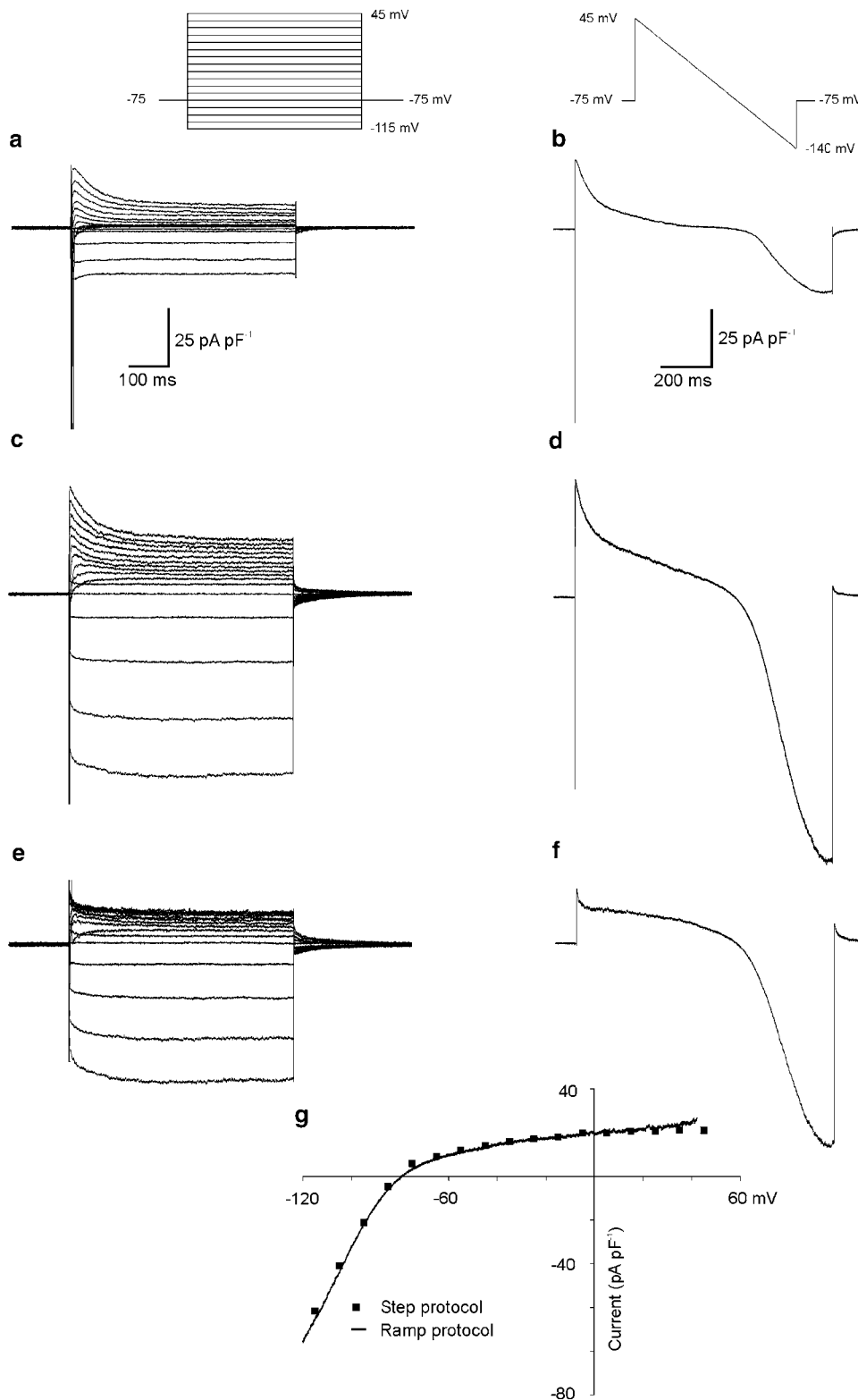
Figure 2 Properties of IKACh in a myocyte from adult mouse atrium. The left and right panels show K^+ current changes in a single right atrial myocyte elicited by a series of voltage clamp steps and voltage ramp protocols (see insets at top). (a, b) Currents recorded under control conditions. The interaction of several voltage- and time-dependent K^+ currents, as well as voltage- and time-dependent Na^+ current, is apparent. Superfusion with 10 μM CCh (c, d) caused a substantial increase in K^+ current as judged by both protocols. Difference currents (e, f) derived by subtracting the currents under control conditions from those in the presence of CCh yield an estimate of IKACh. Panel g demonstrates the close similarity between the $I-V$ relations of the difference currents measured using these two different voltage clamp protocols.

were used throughout the remainder of the study to measure IKACh, as ramps could be applied more often (once every 10 s) than multistep protocols. We also wished to determine whether there might be basal activation of IKACh under the present recording conditions. We recorded whole cell currents in response to the ramp protocol before and during superfusion of the selective IKACh blocker, tertiapin (300 nM; Alamone Labs, Jerusalem, Israel). We observed no effect of tertiapin on basal whole cell K^+ current recorded in four myocytes, and conclude that IKACh is not activated in the absence of muscarinic or adenosine A1 receptor agonists.

In Figure 3, an example of the effect of maximal activation of IKACh on the firing threshold, AP waveform and RMP in an atrial myocyte is presented. Superfusion with $10 \mu M$ CCh caused a hyperpolarisation of the membrane potential and an increase in the amount of current needed to bring the myocyte to threshold. In this myocyte, 0.4 nA was required to depolarise the membrane sufficiently to fire APs under control conditions, whereas 0.9 nA was required following superfusion with CCh. The duration of the AP was also substantially reduced by $10 \mu M$ CCh. Mean $\pm$ s.e.m. data on the effects of CCh on membrane potential, threshold current and AP duration is detailed in Table 1 (see below).

Figure 3b shows results from experiments carried out to identify the K^+ current due to IKACh during a mouse AP. A ramp protocol from 30 to $-75 mV$ lasting 50 ms was used to simulate APs in atrial myocytes (inset). This stimulus was applied at 1 Hz, before and during the superfusion of $10 \mu M$ CCh. The results presented are averages of the final 30 traces of protocols that comprised 60 stimuli at 1 Hz. The addition of CCh to the myocyte caused a substantial increase in the amount of current activated by the ramp.

Comparison of IKACh in left and right atrium and in SA node

The experiments in Figures 4 and 5 were conducted to address the question: are there differences in the maximum amount of IKACh that can be activated in myocytes from left *versus* right atrium. The amplitude of IKACh was measured by subtracting currents during a ramp protocol under control conditions from those recorded when the effect of a ligand that maximally activates IKACh had reached steady state. We found that the amplitude of IKACh activated by a maximal dose of CCh $(10 \mu M)$ was significantly larger at two arbitrarily chosen membrane potentials, -50 and $-100 mV$, in the right atrium *versus* the left atrium (Figure 5). We therefore attempted to determine whether the underlying cause of this current gradient was differences in the expression density of muscarinic receptors, or whether there were differences at some point downstream of the ligand–receptor complex, possibly at the K^+ channels themselves. To examine this possibility, the effects of another ligand at muscarinic receptors (ACh, $10 \mu M$) and another activator of IKACh (adenosine, $100 \mu M$), which binds A_1 receptors, were studied. To do this, it was necessary to establish that adenosine, at a dose that maximally activates IKACh, activates the same K^+ current that CCh does. In the experiment shown in Figure 4, a single myocyte from left atrium was superfused with $100 \mu M$ adenosine, followed by wash of adenosine, followed by $10 \mu M$ CCh. Adenosine and CCh activated a K^+ current with very similar amplitudes and $I-V$ relations.
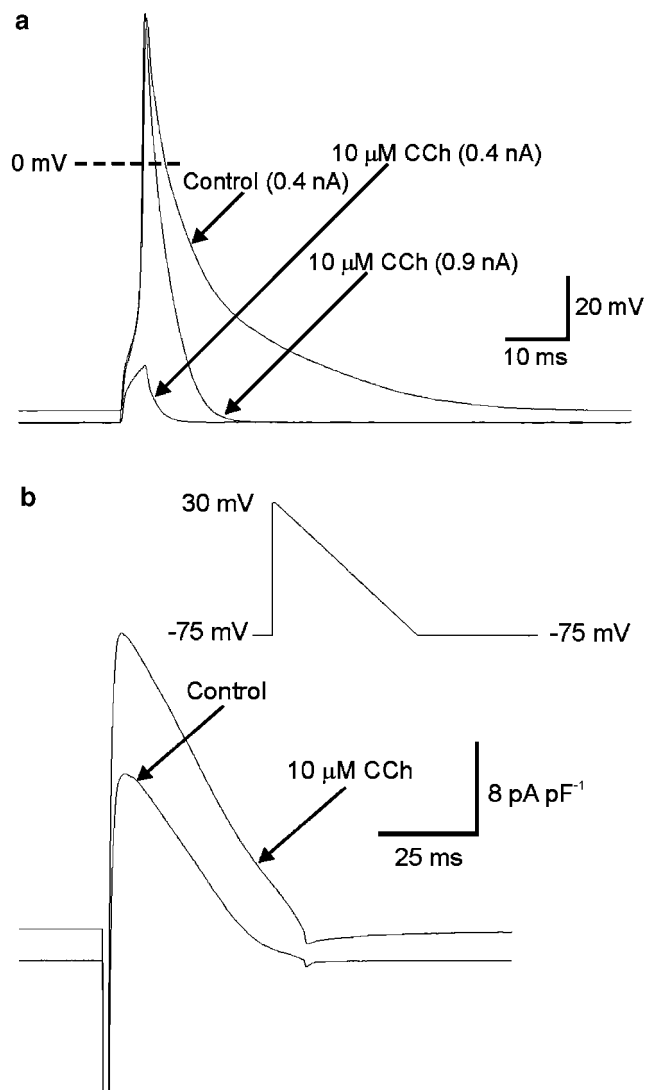

Figure 3 Effect of CCh of action potential (AP) threshold and waveform. (a) APs were recorded from a single mouse atrial myocyte in response to 0.4 nA stimuli applied at 1 Hz. Superfusion of the myocyte with $10 \mu M$ CCh caused a marked hyperpolarisation of the resting membrane potential, and a large increase in the amount of current needed to evoke an AP. When the stimulus was increased to 0.9 nA, APs could again be reliably evoked but their durations were greatly reduced. (b) A hyperpolarising voltage ramp from 30 to $-75 mV$ lasting 50 ms (inset) was used to simulate an atrial AP. These ramp waveforms were applied at 1 Hz before and during superfusion of $10 \mu M$ CCh. During superfusion of CCh, outward current increased at all membrane potentials.

Figure 5 presents mean $\pm$ s.e.m. data from experiments that compared the effects of two muscarinic receptor agonists, CCh and ACh, and an A_1 receptor agonist, adenosine, on myocytes from left and right atrium. Only a single agonist was applied to any of the myocytes in this analysis in order to exclude any possible confounding effects of desensitisation of the IKACh response. Note the significant striking difference in the amplitude of IKACh that can be activated in right and left atrial myocytes. In the right atrium, there is almost twice as much K^+ current as in left atrium at each voltage selected. This difference in current amplitude between right and left atrial myocytes was statistically significant in response to each

Table 1 Comparison of the effects of superfusion of $10\,\mu M$ CCh on action potential properties of single myocytes from left (LA; $n = 11$) and right (RA; $n = 12$) atria. Action potentials were evoked at room temperature at a frequency of 1 Hz. The values before and during superfusion of CCh were compared using two-tailed paired Student's t-tests; difference values were compared using two-tailed unpaired Student's t-tests

	Control	*$10\,\mu M$ CCh*	*Difference*
APD_{50}, LA (ms)	8.1 ± 1.6	3.5 ± 0.3*	4.8 ± 1.4
APD_{50}, RA (ms)	11.3 ± 2.6	2.6 ± 0.2*	9.2 ± 2.7
APD_{90}, LA (ms)	33.2 ± 5.3	10.3 ± 1.7**	23.8 ± 4.0***
APD_{90}, RA (ms)	57.6 ± 7.3	5.6 ± 0.8**	52.6 ± 7.7
RMP, LA (mV)	-70.7 ± 1.9	-75.9 ± 1.0**	5.2 ± 1.0
RMP, RA (mV)	-68.3 ± 1.4	-72.8 ± 1.0**	4.8 ± 0.7
AP threshold, LA (nA) $n = 9$	0.41 ± 0.016	1.0 ± 0.1**	0.6 ± 0.1
AP threshold, RA (nA) $n = 10$	0.39 ± 0.015	1.2 ± 0.2**	0.8 ± 0.2

*$P < 0.05$ *versus* control.
**$P < 0.005$ *versus* control.
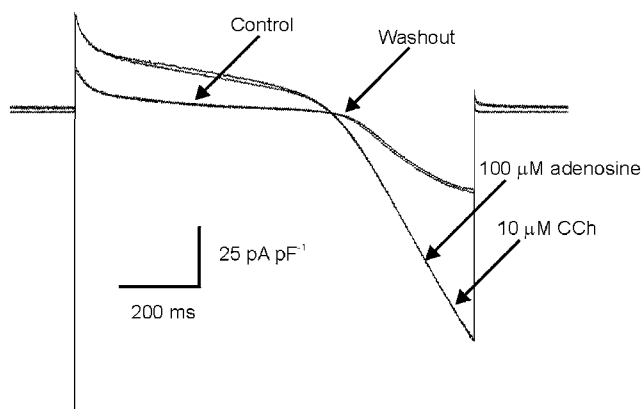***$P < 0.05$ *versus* RA.

Figure 4 Comparison of the effect of adenosine and CCh on K^+ current in a mouse atrial myocyte. Raw data from a voltage clamp experiment which demonstrates that adenosine and CCh activate a current with very similar voltage-dependence and amplitude.

Figure 5 Comparison of IKACh current density between left and right atrial myocytes. The K^+ currents activated in response to a maximal dose of either CCh, ACh or adenosine at -50 and $-100\,mV$ are compared. Regardless of the ligand used or receptor activated, significantly more current was recorded during maximal activation of IKACh in right atrial myocytes than left atrial myocytes.

agonist, which indicates that the gradient of IKACh is independent of the receptor that the agonists bind.

Table 1 presents mean$\pm$s.e.m. data from experiments in which the effect of the gradient of IKACh density on AP properties in single myocytes from both atria was examined. AP characteristics were recorded before and during the application of $10\,\mu M$ CCh. Superfusion of CCh significantly decreased APD_{50} ($P < 0.05$) and APD_{90} ($P < 0.005$) in myocytes from both atria. In addition, the RMPs of myocytes from both atria were hyperpolarised significantly in the presence of CCh ($P < 0.005$), and superfusion of CCh caused an increase ($P < 0.005$) in the amount of current required to reach threshold. We also compared the effect of CCh on each of these parameters between left and right atrial myocytes. The only parameter that was significantly different between left and right atria was the effect on APD_{90}, where CCh caused significantly more shortening of right atrial APs.

The SA node of many species is more densely innervated by cholinergic nerve terminals than the rest of the right atrium, and the right atrium in turn is more densely innervated than the left atrium (reviewed by Loffelholz & Pappano, 1985). We hypothesised that the gradient of IKACh expression between left and 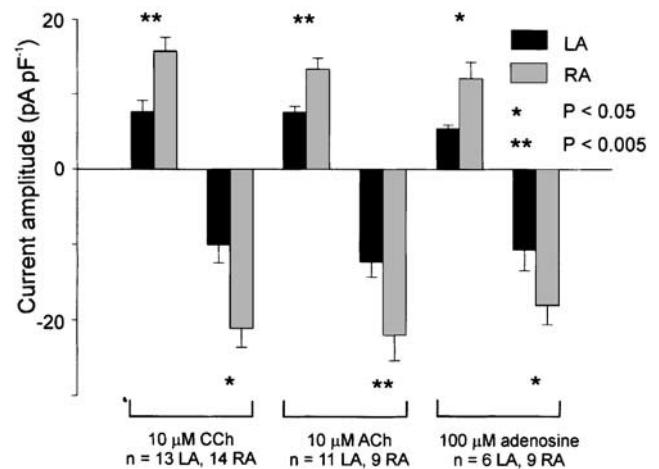right atrium might reflect the gradient of innervation of the atria by cholinergic parasympathetic nerve terminals. A prediction of this hypothesis is that the SA node, which receives significantly more parasympathetic innervation than the right and left atrium, would have more IKACh than either atrium. Figure 6 shows data which suggest that this is the case. Panel a is an $I-V$ relation of $10\,\mu M$ CCh-activated difference current in an SA node myocyte which demonstrates that IKACh in this cell is very similar to that recorded in right and left atrium. Panel b compares IKACh current in each myocyte as well as mean$\pm$s.e.m. data at $-50\,mV$ from 21 SA node cells with data from left and right atrial myocytes. CCh ($10\,\mu M$) activated significantly ($P < 0.005$) more current in SA node myocytes than in left or right atrial myocytes at $-50\,mV$.

Discussion

Results from this study provide strong evidence for a gradient of IKACh current density across mouse atria. This gradient is

not dependent on whether this K^+ current is activated by muscarinic receptors, as an identical gradient of adenosine-dependent K^+ current was also observed. An interesting feature of our data is that the amplitudes of IKACh activated by muscarinic agonists and A_1 agonists were virtually identical. These results differ from previous papers which reported that maximal activation of muscarinic receptors led to substantially larger IKACh than maximal activation of A_1 receptors in myocytes from guinea-pig, rat and human atria (Kurachi *et al.*, 1986; Bunemann & Pott, 1995; Takano & Noma, 1997; Dobrev *et al.*, 2000; Wellner-Kienitz *et al.*, 2000), and suggest that species-dependent differences in G-protein signal transduction efficiency may be involved.

Activation of IKACh caused a significant hyperpolarisation of the RMP in myocytes from both atria. However, maximal activation of IKACh did not hyperpolarise the RMP to the estimated E_K of $-82\,mV$ (Table 1). The RMP of atrial myocytes is determined by the interaction of several time-independent background, pump and exchanger currents (Nygren *et al.*, 1998). Under control conditions, the presence of IK_1 inward rectifier K^+ current is not sufficient to hyperpolarise the RMP to E_K because several of the other background currents exert a depolarising influence. It is likely that activation of IKACh also failed to hyperpolarise the RMP to E_K due to these opposing time-independent inward currents.

Superfusion of atrial myocytes with CCh caused marked effects on excitability and AP duration. Action potential duration, along with conduction velocity, is a major determinant of the wavelength of re-entry, and a decrease in AP duration decreases wavelength, which is often proarrhythmic (e.g., Rensma *et al.*, 1988). Although the threshold current increased in response to CCh, hyperpolarisation of the RMP should increase the availability of I_{Na}, leading to an increase in upstroke velocity of the action potential and increased conduction velocity. However, we did not observe any effect of CCh on the maximum $dV\,dT^{-1}$ during action potential upstrokes (data not shown). This may be due to the presence of M1 receptors on mouse atrial myocytes, which are thought to decrease action potential upstroke velocity (Islam *et al.*, 1998), thus counteracting the effect of membrane hyperpolarisation on availability of I_{Na}. The decreases in excitability (estimated by threshold current) and action potential duration in single myocytes observed during the present study were in response to higher concentrations of muscarinic agonist than are likely to be encountered following normal (reflex-activated) vagal nerve stimulation *in vivo*. Nonetheless, the combination of effects of IKACh on myocyte excitability and AP duration, when distributed in a spatially heterogeneous manner, could account for much of the profibrillatory effects of vagal nerve stimulation.

Possible significance

IKACh can be activated by several pertussis toxin-sensitive G-protein-coupled receptors, including Edg-3, A_1 and muscarinic receptors (Yamada *et al.*, 1998; Himmel *et al.*, 2000). Our experimental work focused on muscarinic receptor-mediated activation of IKACh, due to its potential role in vagally induced atrial arrhythmogenesis. However, we acknowledge that muscarinic receptor signalling does not solely involve IKACh; it also decreases intracellular cAMP concentration *via* $G\alpha_i$ subunits, which modulates several membrane conduc-

tances, including voltage- and time-dependent calcium current (I_{Ca}). Indeed, the concentration of muscarinic receptor ligand needed to affect I_{Ca} is lower than the concentration needed to evoke IKACh. This fact and other findings have led some to question the physiological relevance of IKACh to vagal effects on the heart (Campbell *et al.*, 1989; DiFrancesco *et al.*, 1989; Yamada, 2002). On the other hand, recent studies utilising transgenic mice that lack IKACh have lent support to the idea that vagal effects on the heart do involve IKACh activation. Mice that lack either subunit of IKACh (GIRK1 or GIRK4), or G-protein $\beta\gamma$ subunits, had a mild resting tachycardia and exhibited blunted responses to vagal stimulation or A_1 receptor activation (Wickman *et al.*, 1998; Bettahi *et al.*, 2002; Gehrmann *et al.*, 2002). GIRK4 knockout mice also exhibited markedly reduced heart rate variability (Wickman *et al.*, 1998). Re-entrant arrhythmias in ventricles and atria of adult mice
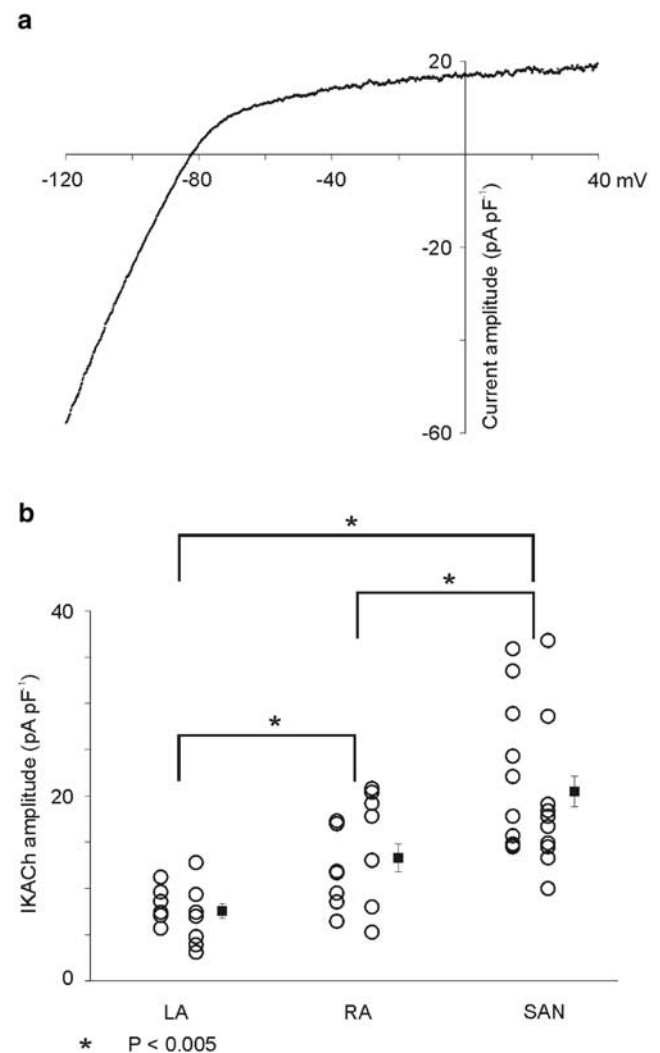
Figure 6 Properties of IKACh in SA node myocytes. (a) The $I-V$ relation of IKACh in an SA node myocyte. Comparison with Figure 2g shows that this $I-V$ relation is very similar to that of atrial myocytes. (b) Comparison of data from individual myocytes (circles) plus mean $\pm$ s.e.m. data (filled squares) for maximal IKACh current density at $-50\,mV$ in SA node myocytes with data from left and right atrial myocytes. IKACh current density is significantly larger in SA node myocytes than both left and right atrial myocytes. Also noteworthy is the degree of cell-to-cell variability of IKACh current density within both atria and within the SA node.

have recently been described (Vaidya *et al.*, 1999; Wakimoto *et al.*, 2001). Wakimoto *et al.* (2001) found that atrial re-entry could be evoked only in the presence of CCh. Moreover, GIRK4 gene knockout siblings, which lack IKACh, did not exhibit atrial re-entry (Kovoor *et al.*, 2001). Similar findings were reported from studies of mice that lacked G-protein $\beta\gamma$ subunits (Gehrmann *et al.*, 2002). These findings show that activation of IKACh in adult mice may play a significant role in the ability of the vagus nerve to regulate heart rate and facilitate atrial arrhythmias.

It has been well established that the anatomic pattern of parasympathetic innervation of the atria is heterogeneous (Loffelholz & Pappano, 1985). This heterogeneity exists at the microscopic level within each atrium, a trend that is mirrored by the variability of IKACh amplitudes observed within both atria in the present study (Figure 6). In addition, the distribution of parasympathetic nerve terminals is more dense in the SA node than in the rest of the right atrium, and the right atrium has more plentiful parasympathetic nerve terminals than the left atrium (e.g. Brown, 1976), which our data indicate is also mirrored by the distribution of IKACh within each region (Loffelholz & Pappano, 1985). The question of whether there might be a causal link between a dense cholinergic innervation and a high expression of atrial IKACh requires further investigation. As the gradient of IKACh amplitude does not appear to be receptor-dependent, we suggest that larger IKACh is due to more plentiful expression of the ion channel subunits, G-protein subunits or interacting intracellular second messengers (Yamada *et al.*, 1998; Fujita *et al.*, 2000). Further studies involving measurements of expression levels of these proteins are required to identify the underlying cause of this IKACh current gradient.

Several recent investigations have lent support to the idea that heterogeneity in the pattern of innervation of the atria can contribute to the ability of vagal nerve stimulation to initiate re-entrant atrial tachyarrhythmias, in part by increasing dispersion of refractoriness within atria (Olgin *et al.*, 1998; Hirose *et al.*, 2002a, b). In addition to the innervation of the atria and the SA node being spatially heterogeneous,

transmitter release at any given autonomic varicosity is a low probability event (Hirst *et al.*, 1996). Thus, repeated identical presynaptic stimuli in a single autonomic axon will result in many different spatial neurotransmitter release profiles with each successive stimulus. The spatial heterogeneity of vagal effects is also superimposed on a heterogeneity of voltage- and time-dependent potassium currents expressed in individual atrial myocytes. Recent work from our laboratory has demonstrated that left atrial myocytes of mice have larger ultra-rapid delayed rectifier and inward rectifier K^+ currents than right atrial myocytes (Lomax *et al.*, 2003). This gradient of voltage- and time-dependent K^+ currents resulted in shorter action potential durations in left atrium compared to right atrium. The complex interactions between expression of voltage- and time- dependent currents (many of which are sensitive to autonomic neurotransmitters), varying levels of IKACh expression and spatial heterogeneity of nerve terminal distribution enables the autonomic nervous system to alter atrial refractoriness in a nonuniform manner that may occasionally promote re-entry (Alessi *et al.*, 1958). In this context, it is interesting to note that recent studies have found evidence of decreased IKACh amplitude, and decreased atrial expression of IKACh channel subunits in patients that have chronic atrial fibrillation (Brundel *et al.*, 2001a, b; Dobrev *et al.*, 2001; 2002).

In summary, the present study presents the first evidence for heterogeneity of a specific G-protein-gated K^+ current in mammalian atria. These data indicate that the spatiotemporal effects of vagus nerve activity on cardiac function are more complex than previously thought.

References

ALESSI, R., NUSYNOWITZ, M., ABILDSKOV, J.A. & MOE, G.K. (1958). Nonuniform distribution of vagal effects on the atrial refractory period. *Am. J. Physiol.*, **194**, 406–410.

BETTAHI, I., MARKER, C.L., ROMAN, M.I. & WICKMAN, K. (2002). Contribution of the Kir3.1 subunit to the muscarinic-gated atrial potassium channel IKACh. *J. Biol. Chem.*, **277**, 48282–48288.

BOUTJDIR, M., LE HEUZEY, J.Y., LAVERGNE, T., CHAUVAUD, S., GUIZE, L., CARPENTIER, A. & PERONNEAU, P. (1986). Inhomogeneity of cellular refractoriness in human atrium: factor of arrhythmia? *Pacing Clin. Electrophysiol.*, **9**, 1095–1100.

BROWN, O.M. (1976). Cat heart acetylcholine: structural proof and distribution. *Am. J. Physiol.*, **231**, 781–785.

BRUNDEL, B.J., VAN GELDER, I.C., HENNING, R.H., TIELEMAN, R.G., TUINENBURG, A.E., WIETSES, M., GRANDJEAN, J.G., VAN GILST, W.H. & CRIJNS, H.J. (2001a). Ion channel remodeling is related to intraoperative atrial effective refractory periods in patients with paroxysmal and persistent atrial fibrillation. *Circulation*, **103**, 684–690.

BRUNDEL, B.J., VAN GELDER, I.C., HENNING, R.H., TUINENBURG, A.E., WIETSES, M., GRANDJEAN, J.G., WILDE, A.A., VAN GILST, W.H. & CRIJNS, H.J. (2001b). Alterations in potassium channel gene expression in atria of patients with persistent and paroxysmal atrial fibrillation: differential regulation of protein and mRNA levels for K+ channels. *J. Am. Coll. Cardiol.*, **37**, 926–932.

BUNEMANN, M. & POTT, L. (1995). Down-regulation of A1 adenosine receptors coupled to muscarinic K+ current in cultured guinea-pig atrial myocytes. *J. Physiol.*, **482**, 81–92.

CAMPBELL, G.D., EDWARDS, F.R., HIRST, G.D. & O'SHEA, J.E. (1989). Effects of vagal stimulation and applied acetylcholine on pacemaker potentials in the guinea-pig heart. *J. Physiol.*, **415**, 57–68.

COUMEL, P. (1996). Autonomic influences in atrial tachyarrhythmias. *J. Cardiovasc. Electrophysiol.*, **7**, 999–1007.

DASCAL, N., SCHREIBMAYER, W., LIM, N.F., WANG, W., CHAVKIN, C., DIMAGNO, L., LABARCA, C., KIEFFER, B.L., GAVERIAUX-RUFF, C. & TROLLINGER, D. (1993). Atrial G protein-activated K+ channel: expression cloning and molecular properties. *Proc. Natl. Acad. Sci. USA*, **90**, 10235–10239.

DIFRANCESCO, D., DUCOURET, P. & ROBINSON, R.B. (1989). Muscarinic modulation of cardiac rate at low acetylcholine concentrations. *Science*, **243**, 669–671.

DOBREV, D., GRAF, E., WETTWER, E., HIMMEL, H.M., HALA, O., DOERFEL, C., CHRIST, T., SCHULER, S. & RAVENS, U. (2001). Molecular basis of downregulation of G-protein-coupled inward rectifying K(+) current (I(K,ACh)) in chronic human atrial fibrillation: decrease in GIRK4 mRNA correlates with reduced I(K,ACh) and muscarinic receptor-mediated shortening of action potentials. *Circulation*, **104**, 2551–2557.

DOBREV, D., WETTWER, E., HIMMEL, H.M., KORTNER, A., KUHLISCH, E., SCHULER, S., SIFFERT, W. & RAVENS, U. (2000). G-Protein beta(3)-subunit 825T allele is associated with enhanced human atrial inward rectifier potassium currents. *Circulation*, **102**, 692–697.

DOBREV, D., WETTWER, E., KORTNER, A., KNAUT, M., SCHULER, S. & RAVENS, U. (2002). Human inward rectifier potassium channels in chronic and postoperative atrial fibrillation. *Cardiovasc. Res.*, **54**, 397–404.

FUJITA, S., INANOBE, A., CHACHIN, M., AIZAWA, Y. & KURACHI, Y. (2000). A regulator of G protein signalling (RGS) protein confers agonist-dependent relaxation gating to a G protein-gated K+ channel. *J. Physiol.*, 341–347.

GEHRMANN, J., MEISTER, M., MAGUIRE, C.T., MARTINS, D.C., HAMMER, P.E., NEER, E.J., BERUL, C.I. & MENDE, U. (2002). Impaired parasympathetic heart rate control in mice with a reduction of functional G protein betagamma-subunits. *Am. J. Physiol.*, **282**, H445–H456.

HIMMEL, H.M., MEYER ZU, H.D., GRAF, E., DOBREV, D., KORTNER, A., SCHULER, S., JAKOBS, K.H. & RAVENS, U. (2000). Evidence for Edg-3 receptor-mediated activation of I(K.ACh) by sphingosine-1-phosphate in human atrial cardiomyocytes. *Mol. Pharmacol.*, **58**, 449–454.

HIROSE, M., CARLSON, M.D. & LAURITA, K.R. (2002a). Cellular mechanisms of vagally mediated atrial tachyarrhythmia in isolated arterially perfused canine right atria. *J. Cardiovasc. Electrophysiol.*, **13**, 918–926.

HIROSE, M., LEATMANORATN, Z., LAURITA, K.R. & CARLSON, M.D. (2002b). Partial vagal denervation increases vulnerability to vagally induced atrial fibrillation. *J. Cardiovasc. Electrophysiol.*, **13**, 1272–1279.

HIRST, G.D., CHOATE, J.K., COUSINS, H.M., EDWARDS, F.R. & KLEMM, M.F. (1996). Transmission by post-ganglionic axons of the autonomic nervous system: the importance of the specialized neuroeffector junction. *Neuroscience*, **73**, 7–23.

ISLAM, M.A., NOJIMA, H. & KIMURA, I. (1998). Muscarinic M1 receptor activation reduces maximum upstroke velocity of action potential in mouse right atria. *Eur. J. Pharmacol.*, **346**, 227–236.

KNOBLOCH, K., BRENDEL, J., PEUKERT, S., ROSENSTEIN, B., BUSCH, A.E. & WIRTH, K.J. (2002). Electrophysiological and antiarrhythmic effects of the novel I(Kur) channel blockers, S9947 and S20951, on left *vs* right pig atrium *in vivo* in comparison with the I(Kr) blockers dofetilide, azimilide, D,L-sotalol and ibutilide. *Naunyn Schmiedebergs Arch. Pharmacol.*, **366**, 482–487.

KOVOOR, P., WICKMAN, K., MAGUIRE, C.T., PU, W., GEHRMANN, J., BERUL, C.I. & CLAPHAM, D.E. (2001). Evaluation of the role of I(KACh) in atrial fibrillation using a mouse knockout model. *J. Am. Coll. Cardiol.*, **37**, 2136–2143.

KRAPIVINSKY, G., GORDON, E.A., WICKMAN, K., VELIMIROVIC, B., KRAPIVINSKY, L. & CLAPHAM, D.E. (1995). The G-protein-gated atrial K+ channel IKACh is a heteromultimer of two inwardly rectifying K(+)-channel proteins. *Nature*, **374**, 135–141.

KUBO, Y., REUVENY, E., SLESINGER, P.A., JAN, Y.N. & JAN, L.Y. (1993). Primary structure and functional expression of a rat G-protein-coupled muscarinic potassium channel. *Nature*, **364**, 802–806.

KURACHI, Y., NAKAJIMA, T. & SUGIMOTO, T. (1986). On the mechanism of activation of muscarinic K+ channels by adenosine in isolated atrial cells: involvement of GTP-binding proteins. *Pflugers Arch.*, **407**, 264–274.

LI, D., ZHANG, L., KNELLER, J. & NATTEL, S. (2001). Potential ionic mechanism for repolarization differences between canine right and left atrium. *Circ. Res.*, **88**, 1168–1175.

LOFFELHOLZ, K. & PAPPANO, A.J. (1985). The parasympathetic neuroeffector junction of the heart. *Pharmacol Rev.*, **37**, 1–24.

LOGOTHETIS, D.E., KURACHI, Y., GALPER, J., NEER, E.J. & CLAPHAM, D.E. (1987). The beta gamma subunits of GTP-binding proteins activate the muscarinic K+ channel in heart. *Nature*, **325**, 321–326.

LOMAX, A.E., KONDO, C.S. & GILES, W.R. (2003). Comparison of time- and voltage-dependent potassium currents in myocytes from the left and right atria of adult mice. *Am. J. Physiol. Heart Circ. Physiol.*. (in press).

MANGONI, M.E. & NARGEOT, J. (2001). Properties of the hyperpolarization-activated current (I(f)) in isolated mouse sino-atrial cells. *Cardiovasc. Res.*, **52**, 51–64.

MANSOUR, M., MANDAPATI, R., BERENFELD, O., CHEN, J., SAMIE, F.H. & JALIFE, J. (2001). Left-to-right gradient of atrial frequencies during acute atrial fibrillation in the isolated sheep heart. *Circulation*, **103**, 2631–2636.

NATTEL, S. (2002). New ideas about atrial fibrillation 50 years on. *Nature*, **415**, 216–219.

NOMA, A. & TRAUTWEIN, W. (1978). Relaxation of the ACh-induced potassium current in the rabbit sinoatrial node cell. *Pflugers Arch.*, **377**, 193–200.

NYGREN, A., FISET, C., FIREK, L., CLARK, J.W., LINDBLAD, D.S., CLARK, R.B. & GILES, W.R. (1998). Mathematical model of an adult human atrial cell: the role of K+ currents in repolarization. *Circ. Res.*, **82**, 63–81.

OLGIN, J.E., SIH, H.J., HANISH, S., JAYACHANDRAN, J.V., WU, J., ZHENG, Q.H., WINKLE, W., MULHOLLAND, G.K., ZIPES, D.P. & HUTCHINS, G. (1998). Heterogeneous atrial denervation creates substrate for sustained atrial fibrillation. *Circulation*, **98**, 2608–2614.

RENSMA, P.L., ALLESSIE, M.A., LAMMERS, W.J., BONKE, F.I. & SCHALIJ, M.J. (1988). Length of excitation wave and susceptibility to re-entrant atrial arrhythmias in normal conscious dogs. *Circ. Res.*, **62**, 395–410.

SIMMONS, M.A. & HARTZELL, H.C. (1987). A quantitative analysis of the acetylcholine-activated potassium current in single cells from frog atrium. *Pflugers Arch.*, **409**, 454–461.

TAKANO, M. & NOMA, A. (1997). Development of muscarinic potassium current in fetal and neonatal rat heart. *Am. J. Physiol.*, **272**, H1188–H1195.

VAIDYA, D., MORLEY, G.E., SAMIE, F.H. & JALIFE, J. (1999). Reentry and fibrillation in the mouse heart. A challenge to the critical mass hypothesis. *Circ. Res.*, **85**, 174–181.

WAKIMOTO, H., MAGUIRE, C.T., KOVOOR, P., HAMMER, P.E., GEHRMANN, J., TRIEDMAN, J.K. & BERUL, C.I. (2001). Induction of atrial tachycardia and fibrillation in the mouse heart. *Cardiovasc. Res.*, **50**, 463–473.

WELLNER-KIENITZ, M.C., BENDER, K., MEYER, T., BUNEMANN, M. & POTT, L. (2000). Overexpressed A(1) adenosine receptors reduce activation of acetylcholine-sensitive K(+) current by native muscarinic M(2) receptors in rat atrial myocytes. *Circ. Res.*, **86**, 643–648.

WICKMAN, K. & CLAPHAM, D.E. (1995). Ion channel regulation by G proteins. *Physiol. Rev.*, **75**, 865–885.

WICKMAN, K., NEMEC, J., GENDLER, S.J. & CLAPHAM, D.E. (1998). Abnormal heart rate regulation in GIRK4 knockout mice. *Neuron*, **20**, 103–114.

WIRTH, K.J. & KNOBLOCH, K. (2001). Differential effects of dofetilide, amiodarone, and class lc drugs on left and right atrial refractoriness and left atrial vulnerability in pigs. *Naunyn Schmiedebergs Arch. Pharmacol.*, **363**, 166–174.

YAMADA, M. (2002). The role of muscarinic K(+) channels in the negative chronotropic effect of a muscarinic agonist. *J. Pharmacol. Exp. Ther.*, **300**, 681–687.

YAMADA, M., INANOBE, A. & KURACHI, Y. (1998). G protein regulation of potassium ion channels. *Pharmacol. Rev.*, **50**, 723–760.